Sustainable Cities and Society 87 (2022) 104167

Contents lists available at ScienceDirect

Sustainable Cities and Society

journal homepage: www.elsevier.com/locate/scs

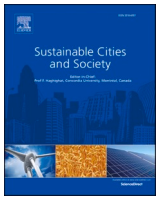

Future urban waterlogging simulation based on LULC forecast model: A case study in Haining City, China

Kexin Yang [a,b], Hao Hou [a,b], Yao Li [c], Yan Chen [a,b], Luoyang Wang [a,b], Pin Wang [a,b], Tangao Hu [a,b,*]

[a] Institute of Remote Sensing and Earth Sciences, Hangzhou Normal University, Yuhangtang Road No. 2318, Hangzhou 311121, China
[b] Zhejiang Provincial Key Laboratory of Urban Wetlands and Regional Change, Hangzhou Normal University, Yuhangtang Road No. 2318, Hangzhou 311121, China
[c] Faculty of Geo-Information Science and Earth Observation (ITC), University of Twente, 7500 AE Enschede, The Netherlands

ARTICLE INFO

Keywords:
LULC change
Urban waterlogging
CLUMondo
InfoWorks ICM

ABSTRACT

As a consequence of rapid urbanization, the pattern of Land Use and Land Cover (LULC) has changed, resulting in a significant increase in the risk of waterlogging. Understanding the relationship between LULC change and urban waterlogging plays an important role in disaster mitigation and prevention. Taking Haining City as an example, the LULC prediction model (CLUMondo) was used to obtain LULC simulation results for 2030.The hydrodynamic model (InfoWorks ICM) was used to simulate future urban waterlogging. The results were as follows: 1) Between 2005 and 2030, the changes in cultivated land and construction land were predicted to be the most obvious. The area of cultivated land was predicted to decrease by 26.62 km^2, and the construction land was predicted to increase by 25.17 km^2. 2) The overall distribution of waterlogged areas and the identified at-risk areas in Haining were shown to be relatively scattered. In 2030, urban waterlogging is predicted to be more serious than in 2020. 3) The reasons for the predicted change in waterlogging are closely related to the transformation of LULC, especially the transformation of cultivated land to construction land. The results provide a basis for scientific research and urban planning to reduce the risk of waterlogging.

1. Introduction

Urbanization is an inevitable consequence of social and economic development (Armeanu et al., 2021). Urban expansion has led to massive population growth (Stokes & Seto, 2019). During the process of urbanization, Land Use and Land Cover (LULC) change not only improves the quality of human life, but also changes the Earth's surface environment, thereby increasing the risk of urban waterlogging disasters and changing the original water cycle process (Shrestha et al., 2018). Urban rain is intensified by urbanization, contributing to the occurrence of extreme rainfall (Oliveira-Junior et al., 2021; Oliveira-Júnior et al., 2022). Urbanization leads to a significant change in the intensity and frequency of flood disasters (Winsemius et al., 2016; Sofia et al., 2017). The frequent occurrence of flood disasters will inevitably have an adverse impact on people's productivity and lives, causing huge economic losses and endangering the safety of residents (Paprotny et al., 2018; Willner et al., 2018).

Disaster risk can be effectively reduced through scientific research and urban planning (Kumar et al., 2022). The premise for alleviating urban waterlogging is to predict and analyze the characteristics of future urban LULC change and the related hydrological effects to provide a basis for scientific research and urban planning (Aich et al., 2016; Silva Cruz et al., 2022).

Predicting future LULC is the basis for waterlogging projections. In the past few decades, researchers have established a variety of simulated prediction models to assess future LULC (Liu et al., 2017; Rahnama, 2021). Deng simulated and predicted the LULC landscape pattern for Mianzhu City using the CA-Markov model (Fu et al., 2022). Mallick used the prediction-adaptation-resilience (PAR) approach to analyze future urban expansion (Mallick et al., 2021). Lin made predictions of LULC through the Future Land Use Simulation (FLUS) model and then predicted future urban waterlogging (Lin et al., 2022). Verburg improved and optimized the Conversion of Land Use and its Effect at Small regional extent (CLUE-S) model by proposing the CLUMondo model (Van Asselen & Verburg, 2013; Ornetsmüller et al., 2021). The CLUMondo model has been widely used in LULC change studies at the

* Corresponding author.
E-mail address: hutangao@hznu.edu.cn (T. Hu).

https://doi.org/10.1016/j.scs.2022.104167
Received 14 June 2022; Received in revised form 4 August 2022; Accepted 3 September 2022
Available online 7 September 2022

regional scale (H. Wang et al., 2021; Bacău et al., 2022).

In recent years, urban LULC change prediction and its hydrological effects have become major hot issues in the field of urban disaster risk management and urban planning (Eum et al., 2016; Wagner et al., 2019). With its advantages of high efficiency, low time consumption, and versatility, the InfoWorks Integrated Catchment Model (ICM) model has been widely used for the evaluation of the current situation regarding urban drainage systems and urban waterlogging risk assessment (Ferguson & Fenner, 2020).

LULC change is one of the main causes of waterlogging, and many scholars have conducted research on the relationship between the two (Zhang et al., 2020). Quan took the Pudong New Area in Shanghai as an example and combined the GIS method and the Soil Conservation Service (SCS) model to evaluate the effect of LULC change on surface runoff as well as the risk of waterlogging caused by precipitation at different intensities (Quan et al., 2010). Wang used the Soil and Water Assessment Tool (SWAT) and the Geographically Weighted Regression Model (GWR) to assess the impact of LULC change on hydrological processes (Wang et al., 2018). Li used improved SCS models and spatial analysis methods to compare the differences in runoff before and after urbanization to assess the impact of urbanization on runoff and marginal effects (Li et al., 2018).

In summary, existing research on urban waterlogging has focused on the relationship between the current situation of LULC change and urban waterlogging. Few studies have explored the impact of future LULC change on urban waterlogging. Quan used the Terraset CA-Markov model to simulate and predict the spatial distribution of LULC in Shanghai in 2030, calculated the level of surface runoff using the SCS model, and predicted and analyzed the impacts of future LULC changes on surface runoff (Quan, 2018). However, the SCS model relies too much on the parameter CN, which can easily cause the final calculation result to differ from the actual situation (Herald, 2022). In addition, the InfoWorks ICM model takes into account the combination of natural factors and urban drainage networks to obtain more accurate results regarding urban waterlogging (Peng et al., 2016). Therefore, the InfoWorks ICM model is more accepted for waterlogging simulation in Haining.

The main objective of this study was to predict the spatial distribution and depth of urban waterlogging in 2030 on the basis of future LULC distribution. In order to accomplish this main purpose, our sub-objectives included: (1) simulation of the LULC for Haining City in 2030; (2) simulation of the urban waterlogging conditions in 2020 and 2030 to analyze the changes in waterlogging; and (3) exploration of the correlation between LULC change and surface runoff.

2. Materials and methods

2.1. Study area

Haining is located in the southern (S) wing of the Yangtze River Delta in China, Hangjiahu Plains, north of Zhejiang Province at 30°15′-30°35′N and 120°18′-120°52′E (Fig. 1). It has a total area of 863 km^2. Haining City is flat and slopes from southwest to northeast. The plains account for 87.94% of the total area, and the low hills are concentrated in the northeast and southeast of Haining. Although Haining is a small city, its urbanization development rate has been relatively fast. From 2000 to 2020, the built-up area of Haining increased from 10.60 km^2 to 55.85 km^2 (JBS, 2021). Therefore, it is a good representative for studies on urbanization. The study area is in a subtropical monsoon climate zone with significant precipitation and obvious seasonal changes. The climate is changeable, and plum rain and typhoons are prone to waterlogging. Typhoon floods, such as "Krosa" in 2007, "Fitow" in 2013, "Lekima" in 2019, and "In-Fa" in 2021 have all brought serious waterlogging disaster losses to Haining. In 2021, the strong typhoon "In-Fa" and super typhoon " Chanthu" positively affected Haining City, bringing heavy rainfall and strong winds. The " In-Fa" typhoon was associated

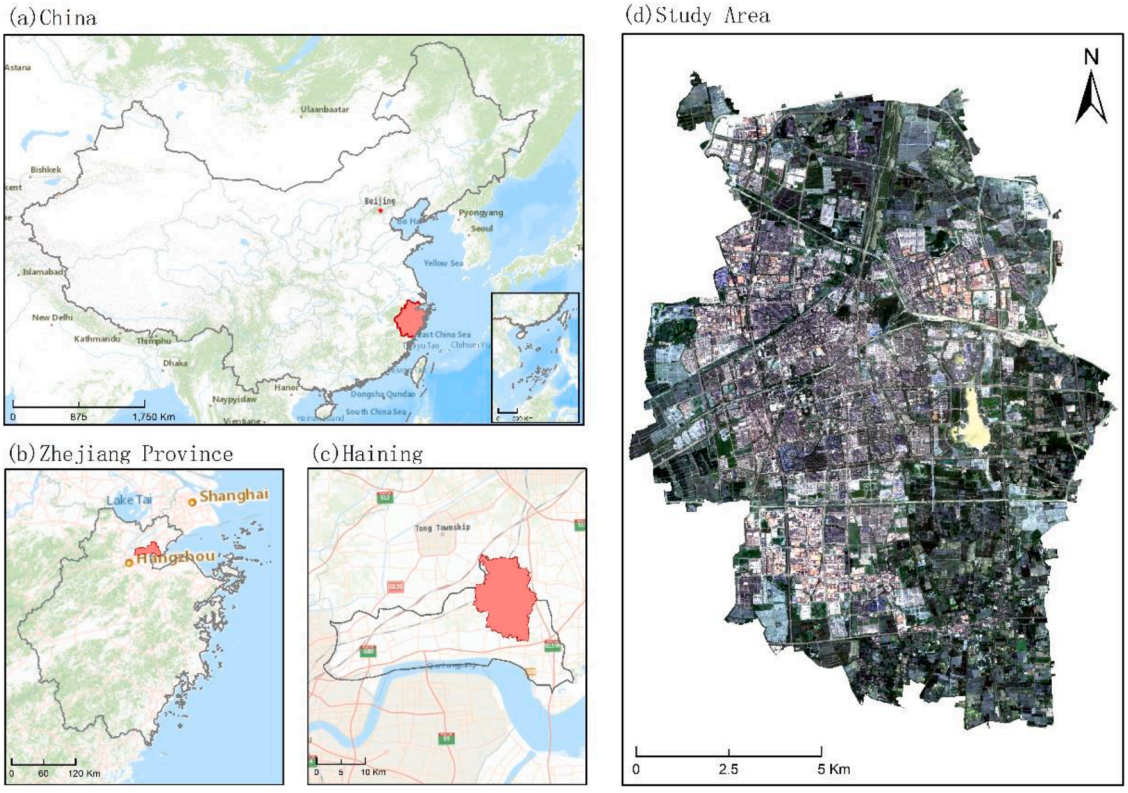

Fig. 1. The geographical location of the study area: (a) Map of China; (b) Location of Zhejiang Province; (c) Location of Haining; (d) Sentinel-2 image of the study area in 2020 displayed in true-color composite (Red—Band 4; Green—Band 3; and Blue—Band 2).

with surface rainfall of 233.8 mm, resulting in a rapid rise in the water level of the river network. (Herald, 2022). This presents a natural advantage for studying urban waterlogging.

2.2. Data

Landsat images, downloaded from the United States Geological Survey (USGS) (http://earthexplorer.usgs.gov/), were employed to obtain the LULC classification data. Sentinel-2 data were derived from the European Space Agency (ESA) (https://www.esa.int). Google Earth images are high-resolution remote sensing stitched data introduced by Maxar. For the high-resolution images, Sentinel-2 data, Google Earth images, and a 1: 5000 Unmanned Aerial Vehicle (UAV) image were used to obtain the validation data for the LULC classification results. The above remote sensing images were pre-processed with radiometric correction, atmospheric correction, and geometric correction.

Advanced Spaceborne Thermal Emission and Reflection Radiometer Global Digital Elevation Model (ASTER GDEM) data were downloaded from the National Aeronautics and Space Administration (NASA) (https://www.nasa.gov). The population density data were downloaded from WorldPop (https://www.worldpop.org/). The slope and aspect of the Digital elevation model (DEM) were extracted using GIS software. Together with railway, river, population density, and county-level residential area data, they were used to determine the driving factors for the LULC predictions.

ASTER GDEM data were also used to simulate urban waterlogging together with the urban drainage network data. The urban drainage network data were simplified without changing the original effect of the network. The numbers of urban drainage nodes and lines were 2916 and 2417 after simplification. Flowmeter measurement records were prepared for verification of the waterlogging simulation results. The detailed data are shown in Table 1.

The above mentioned data were uniformly projected into the WGS_1984_Transverse_Mercator. The spatial resolution was set at 60 m × 60 m according to the needs of the CLUMondo model operation. The data were clipped by the administrative boundary to form the mapping unit.

Table 1
Description of the data used in the study.

Data Type	Time	Resolution	Source
Raster data			
Landsat-5 TM	2005/3/7	30 m	USGS
	2010/5/24	30 m	USGS
Landsat-8 OLI	2015/5/22	30 m	USGS
	2020/5/3	30 m	USGS
Sentinel-2	2020/12/24	10 m	ESA
Google Earth images	2005, 2010, 2015	10 m	USGS
UAV image	2016/6/26	2 m	Haining Natural Resources Bureau
ASTER GDEM	2013	12.5 m	NASA
Population density	2015, 2020	100 m	WorldPop
Vector data			
Administrative boundaries	2021	-	Haining Natural Resources Bureau
railway	2015, 2020	-	Vectorization
river	2015, 2020	-	Vectorization
county-level residential area	2015, 2020	-	Haining Natural Resources Bureau
Urban drainage network	2016	-	Haining City Administration Bureau
Text data			
Flowmeter measurement records	2018	-	Fieldwork
Meteorological precipitation records	2018	-	Haining City Administration Bureau

2.3. Overall workflow

The overall workflow Fig. 2) consisted of four parts: ((1) the LULC classification, where the Landsat remote sensing images were used to obtain the LULC data by the Support vector machine (SVM) method; (2) a simulation of future LULC, where the driving factors and LULC data were entered into the CLUMondo model and the 2030 LULC simulation results were obtained through a regression analysis, parameter setting, and model verification; (3) an urban waterlogging simulation, where LULC data from 2020 and 2030, data on rainfall events, urban drainage network data, and DEM data were entered into the InfoWorks ICM model to obtain urban waterlogging results; and (4) a correlation analysis between LULC change and urban waterlogging. Based on the results of the LULC simulation and urban waterlogging predictions for 2030, the LULC change and urban waterlogging change and their correlation were analyzed, and sustainable development recommendations were made based on the analysis.

2.4. LULC classification

Based on local knowledge and fieldwork, combined with information from similar studies to determine the classification system, LULC was divided into five types: urban green space, construction land, roads and avenues, cultivated land, and water.

SVM technology is widely used in LULC classification. It is highly accurate for the classification of moderate-resolution remote sensing images (Khatami et al., 2016; Hu et al., 2021). In this study, SVM was performed using ENVI® 5.3 by the Harris Corporation and was used to classify the LULC map from 2005, 2010, 2015, and 2020 landsat data.

Validation data were obtained from UAV images, Sentinel-2 data, and Google Earth images through fieldwork and a visual interpretation method. The LULC classification results were verified by the confusion matrix and Pearson Chi-square statistics results (Kafy et al., 2021).

2.5. Simulation of future LULC

2.5.1. Driving factors of LULC change

Geographic factors and socioeconomic factors affect LULC change. Geographic factors play a decisive role in land cover. Topography, slope, aspect, and other natural conditions limit LULC change (Xie et al., 2017; Wu et al., 2021). Socioeconomic factors and related directed development policies also influence LULC change (Stehfest et al., 2019). In this context, seven driving factors—DEM, slope, aspect, distance from the railway, distance from the river, population density, and distance from the nearest county-level residential area—were selected for the simulation.

2.5.2. CLUMondo Construction and Setup

The CLUMondo model is a widely accepted model for accurately predicting future LULC quantities and spatial distributions (Domingo et al., 2021). It is divided into two modules: a non-spatial analysis module and a spatial analysis module. The former makes use of LULC needs, while the latter uses LULC allocation. The simulation of future LULC was achieved through the combination of the two (Debonne et al., 2018).

The specific parameter settings of the CLUMondo model are as follows:

(1) Conversion resistance and conversion matrix.

The conversion matrix was used to detail the LULC type conversion settings. Conversion resistance is related to the reversibility of LULC change. In this study, the conversion matrix and conversion resistance were determined based on historical experience (Fan et al., 2021). After being adjusted to the actual situation, they were set to the number that best suited the study area. The resistance of construction land to other types was set to 0, which indicates that conversion is not allowed, and other LULC types were set to 1, which means that conversion is allowed.

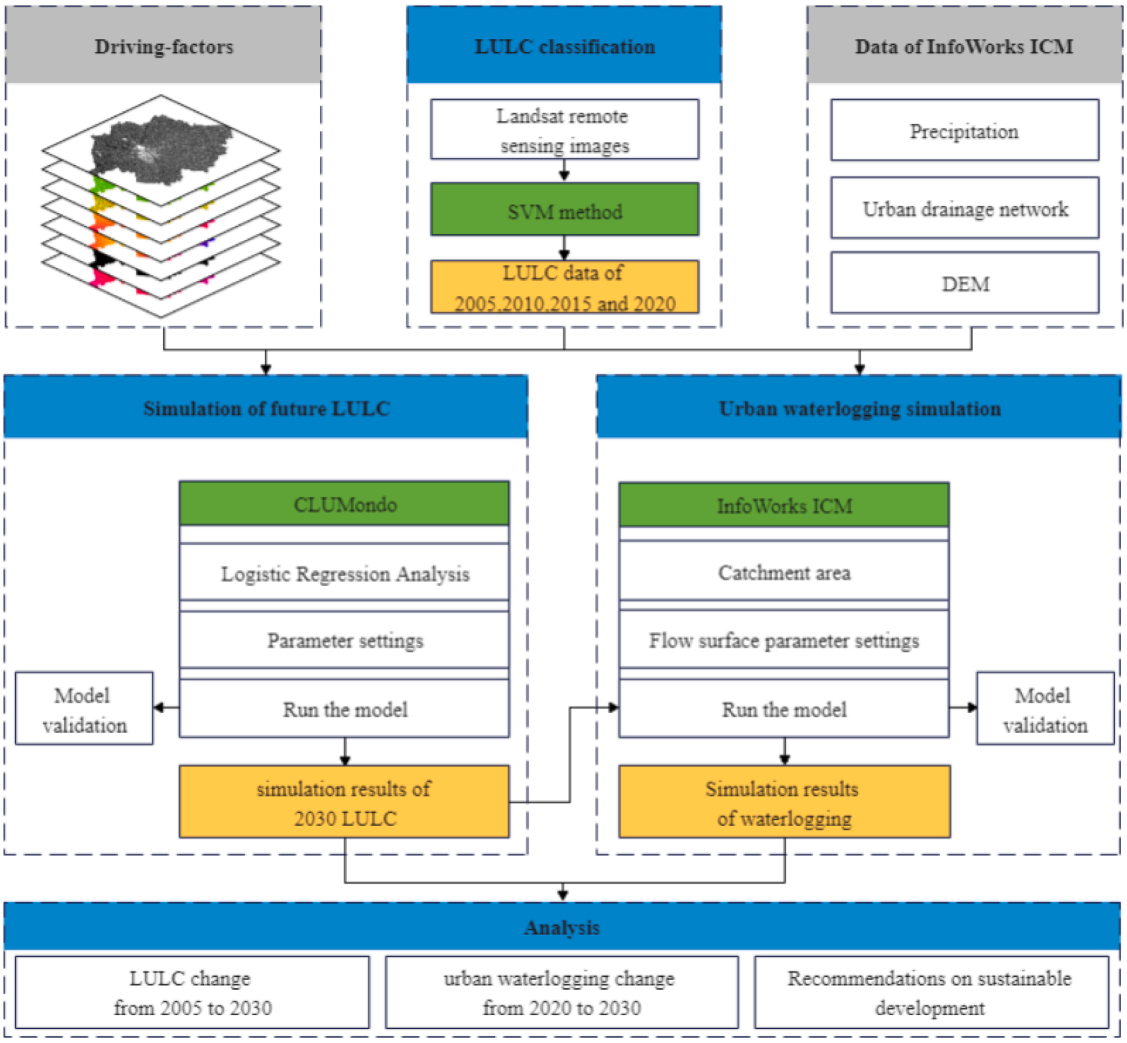

Fig. 2. Overall workflow for the study.

The conversion resistance was set to 0.79 for urban green space, 0.40 for construction land, 0.88 for roads and avenues, 0.25 for cultivated land, and 0.90 for water, where values from 0 to 1 represent conversion from easy to hard.

(2) LULC demand calculation.

Depending on the different research purposes and information provided by different cases, LULC demand can be calculated based on a range of different algorithms (Liao et al., 2022). This study used the historical trend extrapolation method to calculate LULC demand. Future LULC was predicted using the city's actual growth rate from 2005 to 2015.

2.5.3. Logistic Regression Analysis

The logistic regression analysis module is a great differentiator of CLUMondo from other models. The CLUMondo model analyzes the importance of suitability factors by performing a logistic regression analysis (Hu et al., 2020).

The logistic regression analysis calculates the response probability for the figure position features and the driving factors to obtain the function (Gobin et al., 2002).The formula is as follows:

$$Log\left\{\frac{P_i}{(1-P_i)}\right\} = \beta_0 + \beta_1 X_{1i} + \beta_2 X_{2i} + \ldots\ldots + \beta_n X_{ni} \quad (1)$$

where P_i is the probability of the grid element i transforming into a certain LULC type, β is the regression coefficient calculated by the logistic regression analysis of the LULC type and the driving factor, and X represents the driving factor.

Related layers with a relevance of less than 0.8 were selected. On this basis, driving factors with a significance value of less than 0.05 were selected. No more than 7 suitable layers with the highest area under the curve (AUC) value were selected for each LULC type.

2.6. Urban waterlogging simulation

2.6.1. Waterlogging simulation model: InfoWorks ICM

InfoWorks ICM is a drainage model software developed by Innovyze. It is widely used in the assessment of urban drainage systems and the risk assessment of urban waterlogging (Bailey et al., 2020; Yang et al., 2021). InfoWorks ICM can be used to build hydrological and hydraulic models of drainage pipe network systems, and meticulously simulate sewage systems, storm systems, combined drainage systems, and surface diffuse systems. InfoWorks ICM enables more accurate surface flood simulations through the coupling of a 1D hydraulic model to a 2D flood inundation model. The 1D model provides information such as the extent and depth of the water. Two-dimensional models combine complex geometric terrain with evolutionary calculations (T. Zhou et al., 2021).

The basic formulas for calculating the flow of the nullah are the Saint-Venant formulas (Cheng et al., 2017). The specific formulas are as follows:

$$\frac{\sigma A}{\sigma t}+\frac{\sigma Q}{\sigma x}=0 \tag{2}$$

$$\frac{\sigma Q}{\sigma t}+\frac{\sigma}{\sigma x}\left(\frac{Q^2}{A}\right)+gA\left(\cos\theta\frac{\sigma y}{\sigma x}-S_0+\frac{Q|Q|}{K^2}\right)=0 \tag{3}$$

where A is the cross-sectional area of the pipe (m^2), t is time (s), Q is the flow rate (m^3/s), x is the length along the x direction (m), g is gravity (m^2/s), θ is the horizontal angle (degree), y is the depth of the water (m), S_0 is the bed slope, and K is the conveyance.

The following steps in InfoWorks ICM were used to simulate urban waterlogging (H. Zhang et al., 2021). Firstly, the ground elevation model was introduced into InfoWorks ICM. Then, buildings and other obstacles in the city were introduced based on geographic data. A triangulation mesh was automatically generated to calculate the depth and flow rate of water in each triangular mesh. Finally, the depth of the water, the path of the overflow, and the flow rate were obtained.

2.6.2. Model construction

The study area was divided into subcatchments on the basis of the Thiessen polygon method and the actual situation of the region. According to the LULC data, the underlying surface in the study area were generalized into three types: roads, buildings, and other. The runoff calculation was carried out according to the spatial division of the subcatchment area and the surface composition in relation to different flow characteristics. The parameters used are shown in Table 2.

The rainstorm intensity formula for Haining taken from the Hangzhou City Planning Bureau is as follows (OHUZP, 2020):

$$i=\frac{10.101(1+1.057lgP)}{(t+11.3)^{0.682}} \tag{4}$$

where i is the rainstorm intensity(mm/min), P is the return period for rainfall (a), and t is the rainfall duration (min).

Chicago Rainfall was used as the design rain type for the study area. The peak timing ratio r was set to 0.398. Combined with the rainstorm intensity formula, the design rain type was calculated when the return period was 0.5 years, 1 year, 2 years, 5 years, and 10 years.

3. Results

3.1. Model validation results

3.1.1. Validation of the SVM classification results

The confusion matrix results show that the overall classification accuracy in 2005, 2010, 2015, and 2020 was 85.20%, 92.85%, 93.27%, and 88.77%, respectively, which represents a strong validation agreement for the simulated map.

For Chi-square testing, the rejection level was set at a level of significance (LoS) of α= 0.05 with 3 degrees of freedom. The Chi-square value was 7.815. The computed Chi-square values for 2005, 2010, 2015 and 2020 were much lower: 0.732, 0.885, 0.907 and 0.842, respectively. Therefore, the hypothesis was accepted at the 95% confidence level, showing that the classification result and validation data significantly matched each other.

Table 2
Flow surface parameters.

Surface types	Runoff model	Runoff coefficient	Initial losses type	Initial losses/m	Routine model	Routine parameter
Roads	Fixed	0.9	Abs	0.002	SWMM	0.018
Buildings	Fixed	0.8	Abs	0.001	SWMM	0.02
Other	Fixed	0.5	Abs	0.005	SWMM	0.025

3.1.2. CLUMondo model validation

The 2010 LULC data and driving factors were entered into the CLUMondo model, and the conversion resistance, conversion matrix, and LULC demand parameters were used to run the model. Overall AUC values ranged between 0.61 and 0.81, indicating a modest to very good fit. The simulated LULC data for 2015 were obtained, and the Kappa coefficients and confusion matrix (Table 3) were calculated to evaluate the accuracy of the simulation results.

The computed Chi-square value was 0.892, much smaller than the value of 7.815, which indicated that the actual map and simulated map significantly matched each other at the 95% confidence level.

3.1.3. InfoWorks ICM model validation

The flowmeter measurement records collected during rainfall on 3 August 2018 and 20 June 2018 were used to verify the reliability of the model. The results are shown in Fig. 3 and Fig. 4. The Nash–Sutcliffe efficiency coefficient (NES) of the rainfall on 3 August 2018 was 0.991, and the determination coefficient (R^2) was 0.996. The NES on 20 June 2018 was 0.981, and the R^2 value was 0.991. The model fit effect was good, and the water level peak and peak occurrence time simulated by the model matched the measured data.

3.2. LULC simulations for 2005–2030

The results of the 2030 LULC simulation are shown in Fig. 5. The central urban area was predicted to be mainly used for construction, and roads were shown to be interspersed with it. The eastern, southern, and northern marginal areas were predicted to be cultivated land. The Changshan River runs through the city from southeast to northwest. The urban green space was predicted to be small and scattered across the construction land and cultivated land. The area of the city was predicted to continue to grow, and mainly encroach on the area of cultivated land, gradually expanding to the surrounding area. In 2005, the construction land was distributed in the central and southwest areas in a block shape. There was a small area of construction in the cultivated land in the north, east, and south. The western part was mainly cultivated land. In 2010, the construction land had slightly expanded into a blocky area. Other LULC types did not change much. In 2015, the central and southwestern construction land expanded to fill a large area. Small blocks of construction land emerged in the north, and scattered construction land emerged in the West. Water bodies appeared in the central urban area. The number of roads on the east and south sides of the city increased. In 2020, the construction land in the north, west and southwest further developed and grew, and the expansion of the central construction land was not obvious. By 2030, the central, western and southern construction land is predicted to expand to a large area and connect. The distribution of green space in the southeast and northeast is predicted to increase.

The statistical results for each LULC type in the area in 2005, 2010, 2015, 2020, and 2030 are shown in Table 4. The area of cultivated land decreased significantly from 2005 to 2020, while the area of construction land increased. There were small-scale changes of varying degrees in urban green space and roads. Between 2010 and 2015, Haining Juan Lake was artificially built, and the water area increased. The changes in cultivated land and construction land were the most dramatic during the whole process of change. The cultivated land area constantly decreased, and the construction land area increased. The simulation results show that, by 2030, the cultivated land area will be further reduced to 41.18 km^2, a total reduction of 26.62 km^2. The construction land area will further increase to 61.67 km^2, an increase of 25.17 km^2. The water area will increase to 16.11 km^2, an increase of 1.02 km^2. The roads and avenues area will increase to 11.89 km^2, an increase of 2.29 km^2. The urban green space area is predicted to change little, increasing to 23.21 km^2, an increase of 0.02 km^2.

Table 3
The confusion matrix used to test the accuracy of the CLUMondo simulation results.

Observation/ Simulation	Urban green space	Construction Land	Roads and avenues	Cultivated Land	Water	Total	UA
Urban green space	6163	325	178	200	4	6870	95.65%
Construction Land	231	12601	438	1385	43	14698	82.78%
Roads and avenues	7	91	1769	120	1	1988	67.16%
Cultivated Land	15	2053	170	11755	11	14004	86.19%
Water	27	152	79	179	4243	4680	98.63%
Total	6443	15222	2634	13639	4302	42240	-
PA	89.71%	85.73%	88.98%	83.94%	90.66%	-	-
KC	0.814						-
OA	86.48%						-

Note: PA stands for producer's accuracy; UA stands for user's accuracy; OA stands for overall accuracy; KC stands for the Kappa coefficient.

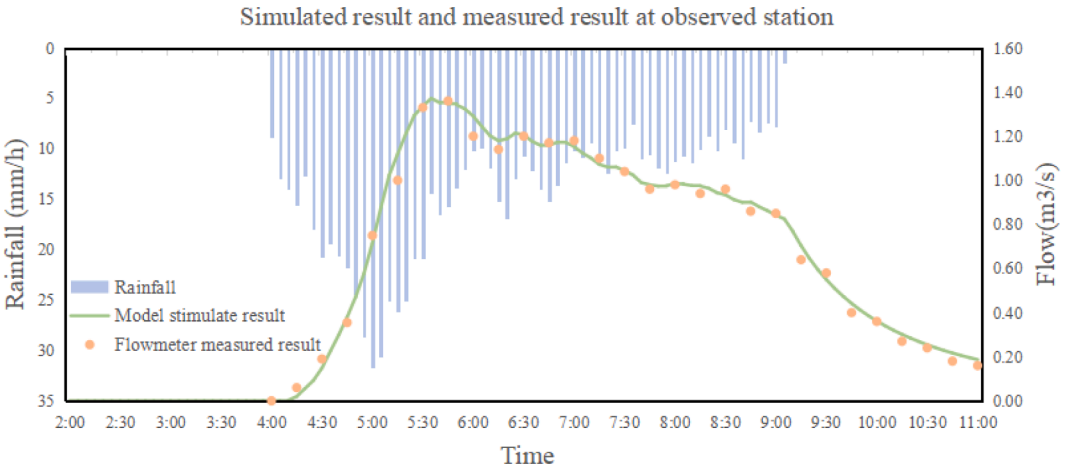

Fig. 3. Results of the rainfall model verification for 3 August.

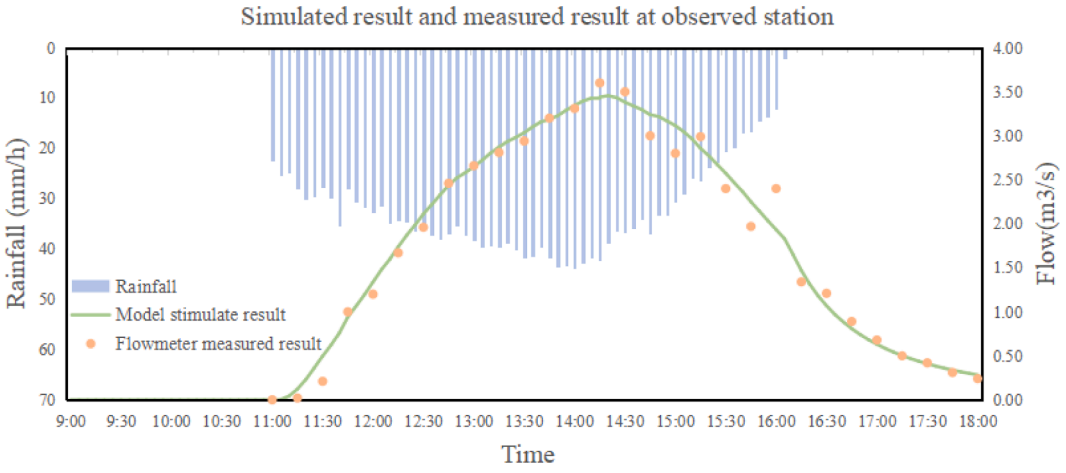

Fig. 4. Results of the rainfall model verification for 20 June.

3.3. Simulation results for urban waterlogging

LULC data, precipitation data, DEM, and drainage network data for 2020 and 2030 were entered into the InfoWorks ICM model to obtain Haining's urban waterlogging results for 2020 and 2030, as shown in Fig. 6. The overall distribution of the waterlogged areas in the study area was found to be relatively scattered with greater distribution around the central business districts. Considering the local conditions and historical records, areas with a depth of more than 1 m were designated as at-risk areas (the red area in the figure). It can be seen that the at-risk areas are also mostly around the central business districts. There are almost no at-risk areas in the north and southeast areas of the city.

The maximum depth and area of water accumulation for each precipitation event in the study area are shown in Table 5. It can be seen that as the return period becomes longer, the intensity of the rainstorm increases, the maximum depth of water accumulation becomes deeper, and the area of water accumulation becomes larger.

Regarding the LULC, in 2020, when the return period increased from 0.5 years to 10 years, the maximum depth of water accumulation increased from 1.376 m to 2.251 m, an increase rate of 63.6%. The area of water accumulation increased from 0.998 km^2 to 3.137 km^2, an increase rate of 214.5%. Regarding the LULC in 2030, when the return

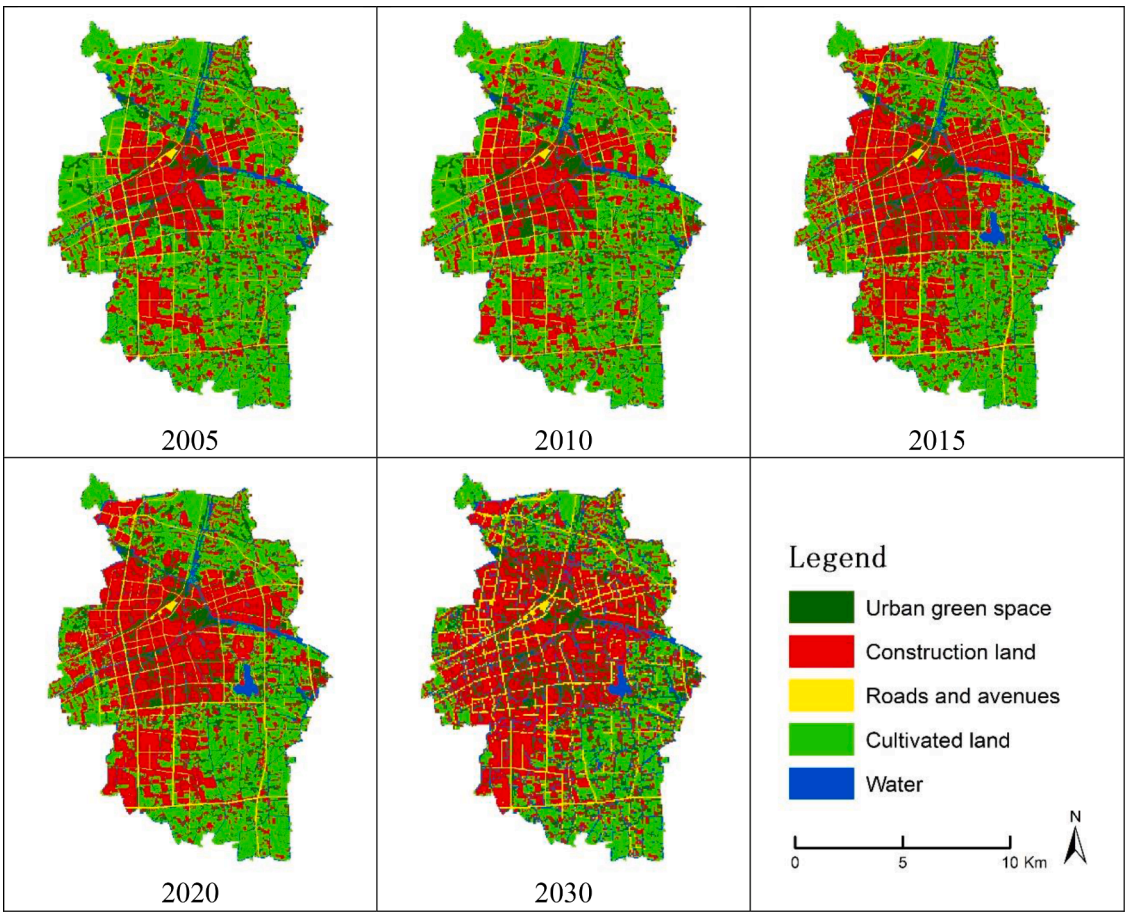

Fig. 5. LULC simulation results for 2005, 2010, 2015, 2020, and 2030.

Table 4
Statistics for the LULC type.

Year	Urban green space	Construction Land	Roads and avenues	Cultivated Land	Water	Total
2005	23.195	36.500	9.601	67.795	14.972	152.064
2010	23.774	41.998	9.706	61.888	14.699	152.064
2015	24.732	52.913	7.157	50.414	16.848	152.064
2020	24.534	55.530	7.171	48.190	16.639	152.064
2030	23.213	61.670	11.892	41.180	16.110	152.064

period was increased from 0.5 years to 10 years, the maximum depth of water accumulation was predicted to increase from 1.513 m to 2.425 m, an increase rate of 60.3%. The area of water accumulation was predicted to increase from 1.126 km^2 to 3.403 km^2, an increase rate of 202.2%.

In addition, the clothing trade in Haining City is very prosperous. In order to better develop the apparel industry, the government concentrated the leather industry enterprise cluster in adjacent areas and started the construction of Haining Garment City in 2005. While the clothing industry has driven the economic and cultural development of Haining City, due to the concentration of impervious water surfaces, the insufficient drainage capacity of pipelines, and other reasons, the city also faces serious waterlogging problems.

The results for waterlogging in the Garment City area regarding the 2030 LULC are shown in Fig. 7. The predicted maximum depth and area of water accumulation for each precipitation event in the Garment City area in 2030 are shown in Table 6. The results show that waterlogging in the region will be concentrated in the central and northwestern parts. When the return period is 0.5 years, only a small area of the northwest was predicted to be at risk. When the return period was 1 year, the predicted at-risk area increased slightly but the growth was not obvious. The number of at-risk areas was not predicted to increase. When the return period was 2 years, the number of areas at risk of water accumulation was predicted to increase with an increase in the area accordingly. When the return period was 5 years, a large area of shallow water accumulation was predicted for the central region, accompanied by an increase in the predicted at-risk area. When the return period was 10 years, the predicted at-risk area increased, but the number of areas did not change. It is sufficient to focus on the northwest region when the return period is 2 years. However, the risk will be greatly increased when encountering precipitation with a return period of 5 years or more. In particular, the depth, area and risk of water accumulation in the central region need to be improved and paid attention to.

3.4. Correlation between urban waterlogging and LULC change

Forty-six watersheds in the study area were obtained using the D8 algorithm. The area of cultivated land converted into construction land and the area of waterlogging growth in each watershed were calculated, and the Pearson correlation coefficient between them was 69.9%. The typical areas of waterlogging change in the southwest of the study area

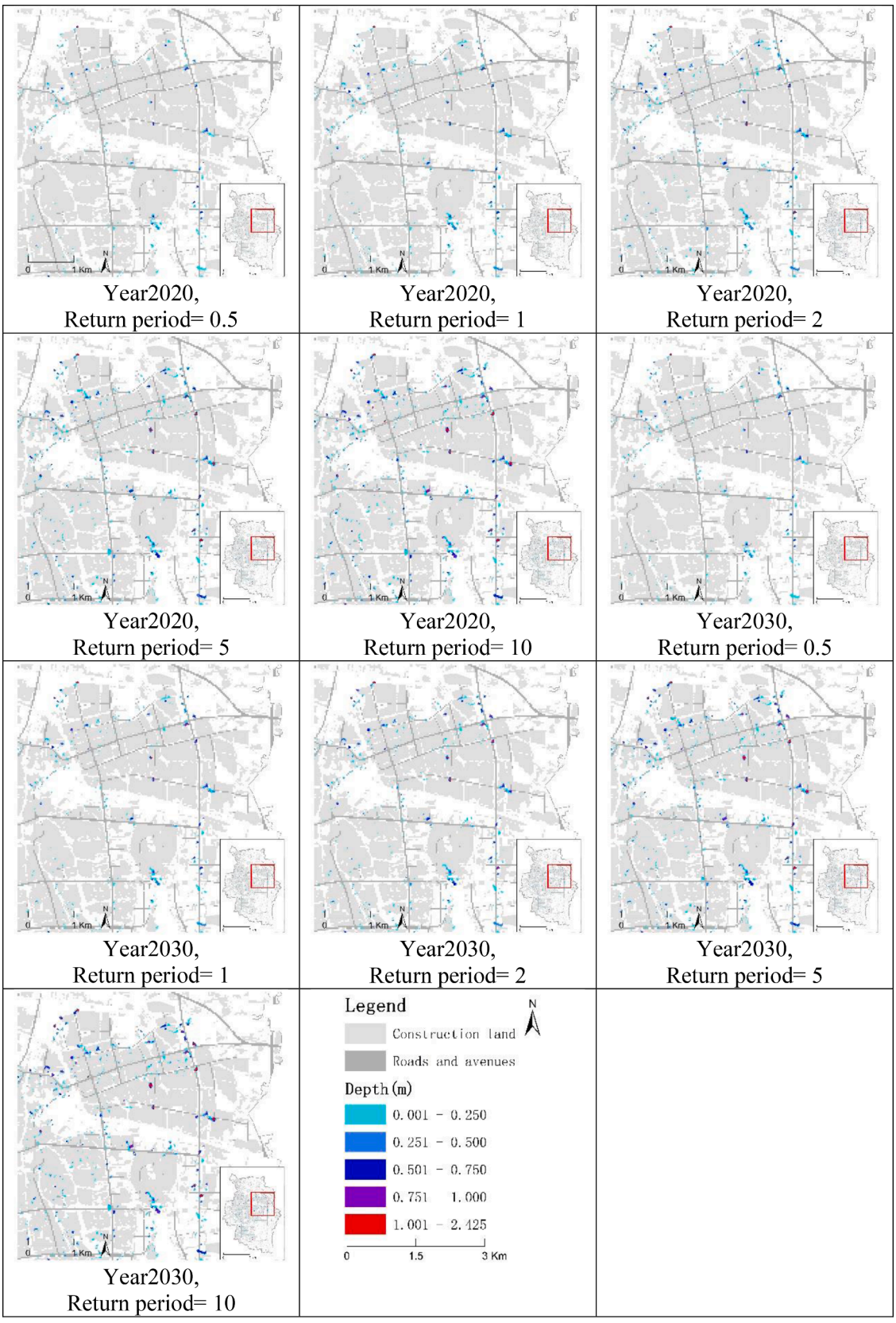

Fig. 6. Urban waterlogging results for 2020 and 2030.

Table 5
Statistical table showing the urban waterlogging results.

Year	Return period/a	Max water depth/m	Average water depth/m	Area of water accumulation/km^2
2020	0.5	1.376	0.187	0.9975
	1	1.718	0.211	1.4750
	2	1.995	0.231	1.9905
	5	2.113	0.259	2.6745
	10	2.251	0.286	3.1370
2030	0.5	1.513	0.196	1.1260
	1	1.927	0.218	1.6835
	2	2.091	0.244	2.2015
	5	2.251	0.277	2.8975
	10	2.425	0.300	3.4030
2030-2020	0.5	0.137	0.010	0.1285
	1	0.209	0.007	0.2085
	2	0.096	0.013	0.2110
	5	0.138	0.017	0.2230
	10	0.174	0.015	0.2660

were further observed and analyzed. The waterlogging situation from 2020 to 2030 is shown in Fig. 8. The LULC transfer matrix is shown in Table 7, and a statistical table of the waterlogging simulation results is shown in Table 8.

For the five types of precipitation events in 2020, although the depth and area of water accumulation in the area showed an increasing trend, no at-risk areas appeared. Regarding the 2030 LULC, no at-risk areas due to precipitation events were predicted in 0.5 years. Small areas of risk will appear in the southwest during periods of precipitation in 1 year. When there is precipitation in 2 years, the at-risk area will increase slightly, and the number of at-risk areas will increase to 3. When there is precipitation in 5 years, the at-risk area will increase significantly. At-risk areas will appear in the north and show a scattered pattern, and the number of risk areas will increase to 7. When precipitation occurs in 10 years, the at-risk area will increase further, and the number of at-risk areas will increase to 8. Combined with the LULC transfer matrix for the region, from 2020 to 2030, 0.374 km^2 of cultivated land is predicted to be converted to construction land and roads, accounting for 55.9% of the cultivated land area. It can be seen that the increased risk of urban waterlogging is closely related to the transformation of cultivated land into construction land.

4. Discussion

4.1. Change of LULC

Increases in features were determined by overlaying polygons from the later year features with those of the earlier year features to be erased. Only portions of the later year features falling outside the earlier year feature boundaries were copied to the output feature class. The feature decrease was determined by looking at the earlier-year features erased by the later year features. The LULC change results obtained through the above methods for 2005 to 2030 are shown in Fig. 9.

According to the simulation results (Fig.9), from 2005 to 2030, the area of cultivated land around the central urban area will greatly reduced. The area of construction land in the same area will increase significantly. This is similar to the results for A0 and A1 in Lithuania (Gomes et al., 2021) but is inconsistent with the results of Cunha's study (Cunha et al., 2021), because the study area in the Prata River basin chosen by Cunha is primarily agricultural, while the area used in this study contains a high-growth city. Prior to urbanization, this study area

Table 6
Statistical table showing urban waterlogging in the Garment City area.

Year ofLULC	Return period/a	Maximum water depth/m	Area of water accumulation/km^2	Area of the risk area/ km^2
2030	0.5	1.174	0.1068	0.0032
	1	1.284	0.1664	0.0041
	2	1.376	0.2826	0.0068
	5	1.476	0.4815	0.0189
	10	1.551	0.5605	0.0213

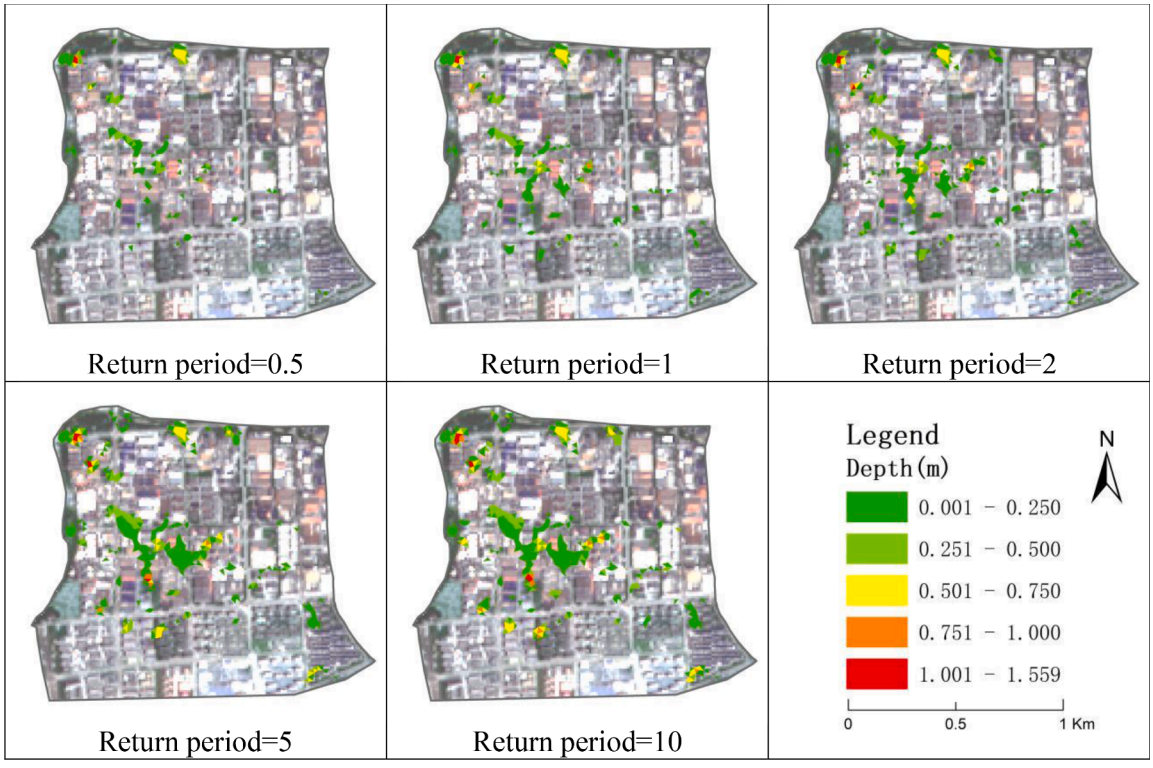

Fig. 7. Results for urban waterlogging in the Garment City area in 2030.

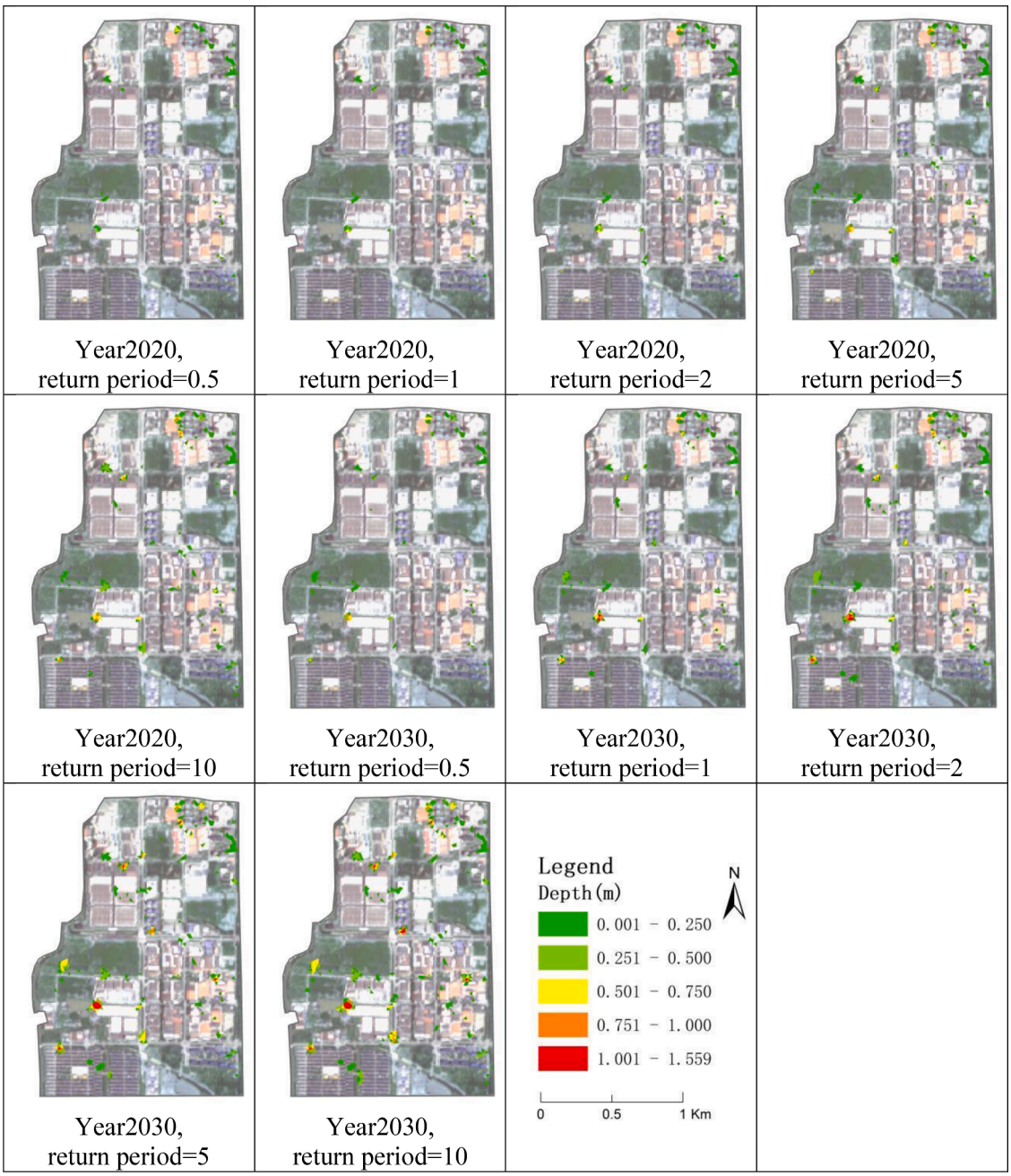

Fig. 8. Results for urban waterlogging in typical areas of the southwest.

Table 7
LULC transfer matrix in typical areas of the southwest.

2020/2030	Urban green space	Construction Land	Roads and avenues	Cultivated Land	Water	Total
Urban green space	0.1584	0	0.018	0	0	0.1764
Construction Land	0	1.4652	0.1692	0	0	1.6344
Roads and avenues	0	0	0.054	0	0	0.054
Cultivated Land	0	0.3024	0.072	0.2952	0	0.6696
Water	0	0	0.0036	0	0.3024	0.306
Total	0.1584	1.7676	0.3168	0.2952	0.3024	2.8404

was mainly cultivated land that was used to provide a living base for local residents. After economic development, the local population no longer depended on agriculture. In order to adapt to the development of the city, the area of cultivated land converted into construction land is predicted to be 23.97 km^2, accounting for 90.1% of the reduced cultivated land and 95.2% of the increase in construction land. Most of the reduced cultivated land will be converted into construction land, and most of the new construction land will occupy cultivated land.

As China enters the 21st century, the national economy has entered a stage of comprehensive and rapid industrialization. The population has

Table 8
Statistical table showing the waterlogging simulation results in typical areas of the southwest.

Year ofLULC	Return period/a	Maximum water depth/m	Area of water accumulation/km^2	Area of the risky area/ km^2
2020	0.5	0.621	0.0263	0.0000
	1	0.757	0.0411	0.0000
	2	0.85	0.0576	0.0000
	5	0.884	0.0754	0.0000
	10	0.973	0.0989	0.0000
2030	0.5	0.916	0.0447	0.0000
	1	1.123	0.0817	0.0014
	2	1.308	0.1077	0.0026
	5	1.492	0.1754	0.0091
	10	1.559	0.2490	0.0146

grown significantly, cities have continued to expand, and the phenomenon of rural areas occupying cultivated land for the building of houses has occurred frequently (Gong et al., 2018). From 2005 to 2010, the area of cultivated land in the study area was rapidly degraded, and the cultivated land area decreased by an average annual amount of 1.18 km^2. Urbanization advanced rapidly, with an average annual increase of 1.10 km^2 in the construction area. Haining City began the construction of a compensation policy for cultivated protection in 2009, but the effect was not good. The compensation incentives were not attractive, resulting in low resident engagement. The income brought by cultivated land and the incentives for cultivated protection were not enough to meet the development needs of residents. The erosion of cultivated land and the growth rate of construction accelerated. From 2010 to 2015, the average annual decrease in cultivated land area was 2.29 km^2, and the average annual increase in construction land was 2.18 km^2. Haining City further established a basic cultivated protection incentive mechanism and a joint responsibility mechanism for cultivated protection, continued to promote farmland protection policies and increased farmland protection incentive funds (Wang et al., 2010; Zhang et al., 2014; Y. Zhou et al., 2021). The phenomenon of construction-induced erosion of cultivated land has been effectively improved. From 2015 to 2020, the average annual decrease in cultivated land area was 0.44 km^2, and the average annual increase in construction land was 0.52 km^2. However, at present, the protection of cultivated land is still not enough prevent its degradation. By 2030, the area of cultivated land is predicted to decrease by an average annual rate of 0.70 km^2, accompanied by an average annual increase in construction area of 0.61 km^2. In short, although Haining has taken measures to protect its cultivated land, the area of cultivated land has still decreased year-by-year, and the construction area has increased year-by-year, and this trend will continue in the future.

In addition, the application of CLUMondo is not limited to the prediction of waterlogging. This model includes the LULC intensity, thereby effectively improving the accuracy of LULC simulation. Therefore, it can be applied to a variety of social and environmental fields related to LULC and sustainable issues, including population research, carbon storage research, and urban planning research (Nie et al., 2020; Domingo et al., 2021; Y. Wang et al., 2021).

4.2. Changes in and causes of urban waterlogging

Under the 2030 LULC situation, the waterlogging situation was predicted to be more severe than in 2020, with a larger area, greater depth, and more at-risk areas, a result that is similar to those of Pal's study conducted in India (Pal et al., 2022). Figs. 5 and 6 show that waterlogging is predicted to be distributed around the central business districts, where there is a drainage pipe network. According to the field work, the drainage pipes here are relatively narrow with insufficient capacity to drain the rainwater away, resulting in siltation of the rainwater. In addition, the terrain is relatively low-lying, and the proportion of impervious water surfaces is high, making rainwater less likely to seep down, causing it to pool in low-lying areas and cause waterlogging. This result is similar to Zhang's discovery in the Chebei Watershed that the uneven topography distribution and LULC have resulted in unevenness in the spatial distribution of waterlogging (M. Zhang et al., 2021). The growth of waterlogging from 2020 to 2030 is also predicted to be mainly located in the above areas. The depth and area of water accumulation in other areas were not obvious. In the north and southeast areas of the city without pipe network distribution, no waterlogging was predicted, a result that differs from previous waterlogging results for Xiamen Island (Liu et al., 2020). However, according to fieldwork, there will also be slight water accumulation in these areas. Because Liu's drainage network was shown to be evenly distributed in the study area, the waterlogging results were also evenly distributed. The InfoWorks ICM model simulation of water accumulation relies on urban drainage network data. Waterlogging occurs only in areas in which urban drainage networks are distributed (Song et al., 2021). In subsequent studies, in order to further improve the accuracy of the InfoWorks ICM model, it is necessary to improve the drainage network data. Combination with other models is also a recommended way to achieve a high level of accuracy.

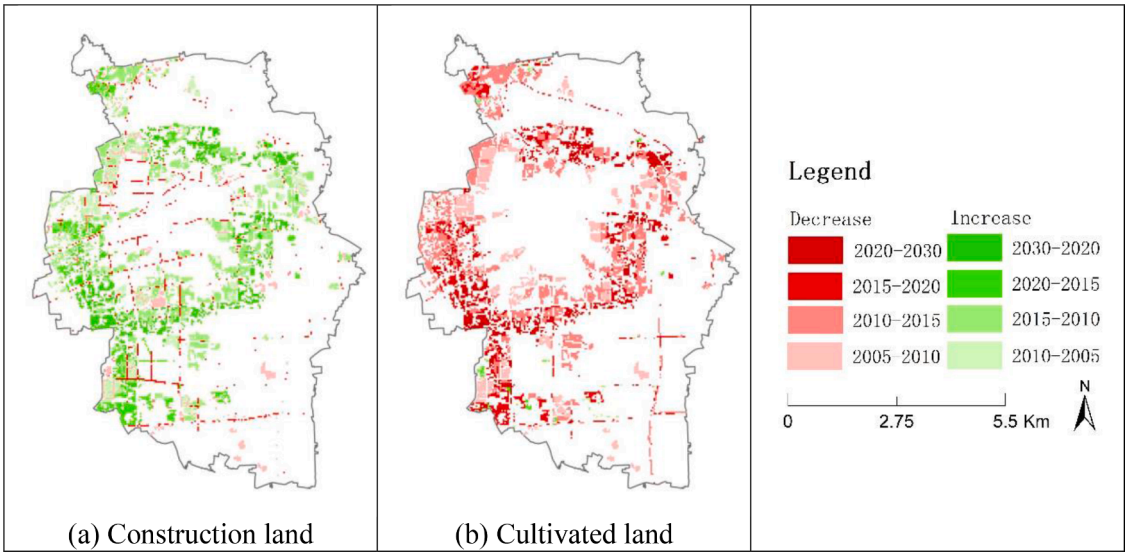

Fig. 9. LULC changes from 2005 to 2030: (a) Change in construction land; (b) Change in cultivated land.

In the Costume City area, in order to carry out centralized commercial development, the area is mainly set up with impervious water surfaces, such as construction land and roads. The impervious water surfaces are concentrated and distributed across a whole block, which is not conducive to the infiltration of water. Xu's study also supports this, since they showed that less surface runoff would be generated in low-density settlement areas in Munich (Xu et al., 2020). Moreover, the area is low-lying and prone to water accumulation. In addition, although there is a pipe network in this area, the number of pipe networks is small, and the distribution is sparse. The diameters of the pipes are mostly 400–600 mm, and the drainage capacity is weak. The above reasons have caused a large area of water accumulation in the Costume City area.

In the typical southwest area, based on the waterlogging results for 2020 and 2030, it can be inferred that the degradation of large areas of cultivated land will cause increases in the depth and area of waterlogging, leading to a serious increase in the risk of waterlogging.

4.3. Recommendations for sustainable development of urban waterlogging based on LULC change

Overall, from 2020 to 2030, the maximum depth and area of water accumulation in the study area is predicted to increase. According to Fig. 6, Fig. 7, and Fig. 9, combined with the high correlation between urban waterlogging and LULC change, it can be seen that the main reason for the serious waterlogging is the transformation of urban green space and cultivated land, especially the reduction of cultivated land. This law also applies to Ren's discovery that urban imperviousness plays an important role in reducing surface runoff (Ren et al., 2020). The area where cultivated land is converted into construction land corresponds to the area in which the depth and area of waterlogging are predicted to increase. Based on this, the following recommendations are made to reduce the increase in urban waterlogging caused by LULC change and promote the sustainable development of cities.

The CLUMondo model and the InfoWorks ICM model have high levels of simulation accuracy. At the global scale, LULC change has brought about serious waterlogging problems (Sterling et al., 2013; Lapointe et al., 2022). Regions can predict future LULC and waterlogging from simulations using these two models. On this basis, urban planning and transformation can be carried out to fundamentally prevent the occurrence of waterlogging. This can provide the foundation for the rational expansion of the city and the deployment of the urban drainage network.

Many scholars have made recommendations for alleviating urban waterlogging Liu et al., 2022; Shahzad et al., 2022). For Haining City, there are the following three targeted recommendations: ((1) Haining City should improve its compensation system for cultivated land protection and severely crack down on the behavior of arbitrarily occupying cultivated land and building houses. Effort should be made to strengthen the control, construction, and encouragement of cultivated land for protection. It is recommended that the area of cultivated land should not be reduced, so that cultivated land protection can be effectively achieved. The construction land growth rate should be controlled, and it is suggested that the rate of urban expansion should be slowed down. (2) New construction land should be scattered to avoid excessive agglomeration in the same area, such as in the Garment City area. If necessary, it is suggested that construction land should be demolished to restore cultivated land. In the case of difficulty in restoring cultivated land, more urban green space should be arranged among the construction land. It is recommended that the degree of construction land dispersion should be increased, and the production of flow should be reduced to alleviate urban waterlogging. (3) Construction land and roads in at-risk areas should be sponge-remodeled. The underlying surface should be optimized to reduce the production of flow. At the same time, it is suggested that the urban drainage network should be optimized and the drainage capacity of the network should be improved to achieve the goal of sustainable urban development. At the same time, the drainage network should be transformed and optimized to improve the drainage capacity and avoid rainwater siltation.

4.4. Limitations and Future Perspectives

Several limitations should be addressed to better understand the results. First, the inconsistency in data years resulted in a decrease in simulation accuracy. In the future, data collected closer together could be used to improve the simulation accuracy. Second, a single simulation scenario was used. Scenarios such as the Intergovernmental Panel on Climate Change (IPCC), economic development, and natural environmental protection should be considered in the future to explore the risk of urban waterlogging in the context of climate change and sustainable urban development. Third, the historical trend extrapolation method used in the calculation of LULC demand is actually a relatively simple functional model. In future research, various factors, like areas restricted from development by the government, could be included to improve the accuracy of the LULC simulation results.

5. Conclusion

Taking Haining City as an example, based on the simulation results of the LULC in 2030, waterlogging in the city was predicted, and the correlation between LULC change and urban waterlogging was discussed. The main conclusions are as follows:

(1) The CLUMondo model applied to Haining has a high level of accuracy for LULC predictions (Kappa coefficient is 0.81, overall classification accuracy is 86.48%). It can lay a solid foundation for following in-depth studies of future LULC conversion trends. The simulation results show that, among the changes in the LULC structure of Haining from 2005 to 2030, the changes in cultivated land and construction land will be the most obvious.

(2) The overall distribution of the waterlogged areas and the identified at-risk areas in Haining were shown to be relatively scattered, with greater distribution around the central business districts. Because there is a drainage pipe network distribution that is not dense, the terrain is relatively low-lying, and the proportion of impervious water surfaces is high. The overall results show that urban waterlogging in 2030 will be more serious than in 2020.

(3) The reasons for the change of waterlogging in Haining City between 2005 and 2030 are closely related to the transformation of LULC, especially the transformation of cultivated land to construction land. The correlation between the two reached 69.9%. In order to alleviate urban waterlogging, it is necessary to improve the compensation system for cultivated land protection. New construction land should be scattered to avoid excessive agglomeration in the same area. It is suggested that cultivated land should be restored as much as possible, and urban green space should be increased.

In summary, this study described a complete process for simulating waterlogging development based on future LULC predictions. The combination of the confusion matrix and Pearson Chi-square statistical methods guarantees the accuracy of future LULC predictions. The accuracy of the waterlogging simulation was verified by the field investigation data. Based on the correlation between LULC development and waterlogging disasters, specific urban planning suggestions were proposed. This process is recommended in other cities with rapid urbanization and severe waterlogging disasters and can provide a basis for the construction of livable cities and sustainable development.

Declaration of Competing Interest

The authors declare that they have no known competing financial interests or personal relationships that could have appeared to influence the work reported in this paper.

Data availability

Data will be made available on request.

References

Aich, V., Liersch, S., Vetter, T., Fournet, S., Andersson, J. C. M., Calmanti, S., van Weert, F. H. A., Hattermann, F. F., & Paton, E. N. (2016). Flood projections within the Niger River Basin under future land use and climate change. *Science of The Total Environment, 562*, 666–677. https://doi.org/10.1016/j.scitotenv.2016.04.021

Armeanu, D. S., Joldes, C. C., Gherghina, S. C., & Andrei, J. V. (2021). Understanding the multidimensional linkages among renewable energy, pollution, economic growth and urbanization in contemporary economies: Quantitative assessments across different income countries' groups. *Renewable and Sustainable Energy Reviews, 142*. https://doi.org/10.1016/j.rser.2021.110818

Bacău, S., Domingo, D., Palka, G., Pellissier, L., & Kienast, F. (2022). Integrating strategic planning intentions into land-change simulations: Designing and assessing scenarios for Bucharest. *Sustainable Cities and Society, 76*. https://doi.org/10.1016/j.scs.2021.103446

Bailey, O., Zlatanovic, L., van der Hoek, J. P., Kapelan, Z., Blokker, M., Arnot, T., & Hofman, J. (2020). A Stochastic Model to Predict Flow, Nutrient and Temperature Changes in a Sewer under Water Conservation Scenarios. *Water, 12*. https://doi.org/10.3390/w12041187

Cheng, T., Xu, Z., Hong, S., & Song, S. (2017). Flood Risk Zoning by Using 2D Hydrodynamic Modeling: A Case Study in Jinan City. *Mathematical Problems in Engineering, 2017*, 1–8. https://doi.org/10.1155/2017/5659197

Cunha, E. R.d., Santos, C. A. G., Silva, R. M.d., Bacani, V. M., & Pott, A. (2021). Future scenarios based on a CA-Markov land use and land cover simulation model for a tropical humid basin in the Cerrado/Atlantic forest ecotone of Brazil. *Land Use Policy, 101*. https://doi.org/10.1016/j.landusepol.2020.105141

Debonne, N., van Vliet, J., Heinimann, A., & Verburg, P. (2018). Representing large-scale land acquisitions in land use change scenarios for the Lao PDR. *Regional Environmental Change, 18*, 1857–1869. https://doi.org/10.1007/s10113-018-1316-8

Domingo, D., Palka, G., & Hersperger, A. M. (2021). Effect of zoning plans on urban land-use change: A multi-scenario simulation for supporting sustainable urban growth. *Sustainable Cities and Society, 69*. https://doi.org/10.1016/j.scs.2021.102833

Eum, H.-I., Dibike, Y., & Prowse, T. (2016). Comparative evaluation of the effects of climate and land-cover changes on hydrologic responses of the Muskeg River, Alberta, Canada. *Journal of Hydrology: Regional Studies, 8*, 198–221. https://doi.org/10.1016/j.ejrh.2016.10.003

Fan, J., Li, Y., Zhu, W., Chen, Y., Li, Y., Hou, H., & Hu, T. (2021). Evaluating the Impact of Mega-Sports Events on Urbanization Focusing on Land-Use Changes Using a Scenario-Based Model. *Sustainability*, 13. https://doi.org/10.3390/su13041649

Ferguson, C., & Fenner, R. (2020). The impact of Natural Flood Management on the performance of surface drainage systems: A case study in the Calder Valley. *Journal of Hydrology, 590*. https://doi.org/10.1016/j.jhydrol.2020.125354

Fu, F., Deng, S., Wu, D., Liu, W., & Bai, Z. (2022). Research on the spatiotemporal evolution of land use landscape pattern in a county area based on CA-Markov model. *Sustainable Cities and Society, 80*. https://doi.org/10.1016/j.scs.2022.103760

Gobin, A., Campling, P., & Feyen, J. (2002). Logistic modelling to derive agricultural land use determinants: A case study from southeastern Nigeria. *Agriculture, Ecosystems and Environment, 89*, 213–228. https://doi.org/10.1016/S0167-8809(01)00163-3

Gomes, E., Inacio, M., Bogdzevic, K., Kalinauskas, M., Karnauskaite, D., & Pereira, P. (2021). Future scenarios impact on land use change and habitat quality in Lithuania. *Environmental Research, 197*, Article 111101. https://doi.org/10.1016/j.envres.2021.111101

Gong, J., Jiang, C., Chen, W., Chen, X., & Liu, Y. (2018). Spatiotemporal dynamics in the cultivated and built-up land of Guangzhou: Insights from zoning. *Habitat International, 82*, 104–112. https://doi.org/10.1016/j.habitatint.2018.10.004

Herald, X. M. (2022). Review of flood prevention and disaster reduction in Haining City in 2021 (in Chinese).

Hu, T., Fan, J., Hou, H., Li, Y., Li, Y., & Huang, K. (2021). Long-term monitoring and evaluation of land development in a reclamation area under rapid urbanization: A case-study in Qiantang New District, China. *Land Degradation and Development, 32*, 3259–3271. https://doi.org/10.1002/ldr.3980

Hu, T., Liu, J., Zheng, G., Zhang, D., & Huang, K. (2020). Evaluation of historical and future wetland degradation using remote sensing imagery and land use modeling. *Land Degradation and Development, 31*, 65–80. https://doi.org/10.1002/ldr.3429

JBS (Jiaxing Bureau of Statistics) Jiaxing Statistical Yearbook. (2021). http://tjj.jiaxing.gov.cn/col/col1512382/index.html (accessed 29 July 2022).

Kafy, A.-A., Naim, M. N. H., Subramanyam, G., Faisal, A.-A., Ahmed, N. U., Rakib, A. A., Kona, M. A., & Sattar, G. S. (2021). Cellular Automata approach in dynamic modelling of land cover changes using RapidEye images in Dhaka, Bangladesh. *Environmental Challenges, 4*. https://doi.org/10.1016/j.envc.2021.100084

Khatami, R., Mountrakis, G., & Stehman, S. V. (2016). A meta-analysis of remote sensing research on supervised pixel-based land-cover image classification processes: General guidelines for practitioners and future research. *Remote Sensing of Environment, 177*, 89–100. https://doi.org/10.1016/j.rse.2016.02.028

Kumar, S., Guntu, R. K., Agarwal, A., Villuri, V. G. K., Pasupuleti, S., Kaushal, D. R., Gosian, A. K., & Bronstert, A. (2022). Multi-objective optimization for stormwater management by green-roofs and infiltration trenches to reduce urban flooding in central Delhi. *Journal of Hydrology, 606*. https://doi.org/10.1016/j.jhydrol.2022.127455

Lapointe, M., Rochman, C. M., & Tufenkji, N. (2022). Sustainable strategies to treat urban runoff needed. *Nature Sustainability*. https://doi.org/10.1038/s41893-022-00853-4

Li, C., Liu, M., Hu, Y., Shi, T., Qu, X., & Walter, M. T. (2018). Effects of urbanization on direct runoff characteristics in urban functional zones. *Science of The Total Environment, 643*, 301–311. https://doi.org/10.1016/j.scitotenv.2018.06.211

Liao, G., He, P., Gao, X., Lin, Z., Huang, C., Zhou, W., Deng, O., Xu, C., & Deng, L. (2022). Land use optimization of rural production–living–ecological space at different scales based on the BP–ANN and CLUE–S models. *Ecological Indicators, 137*. https://doi.org/10.1016/j.ecolind.2022.108710

Lin, J., He, P., Yang, L., He, X., Lu, S., & Liu, D. (2022). Predicting future urban waterlogging-prone areas by coupling the maximum entropy and FLUS model. *Sustainable Cities and Society, 80*. https://doi.org/10.1016/j.scs.2022.103812

Liu, J., Shao, W., Xiang, C., Mei, C., & Li, Z. (2020). Uncertainties of urban flood modeling: Influence of parameters for different underlying surfaces. *Environmental Research, 182*. https://doi.org/10.1016/j.envres.2019.108929

Liu, W., Qian, Y., Yao, L., Feng, Q., Engel, B. A., Chen, W., & Yu, T. (2022). Identifying city-scale potential and priority areas for retrofitting green roofs and assessing their runoff reduction effectiveness in urban functional zones. *Journal of Cleaner Production, 332*. https://doi.org/10.1016/j.jclepro.2021.130064

Liu, X., Liang, X., Li, X., Xu, X., Ou, J., Chen, Y., Li, S., Wang, S., & Pei, F. (2017). A future land use simulation model (FLUS) for simulating multiple land use scenarios by coupling human and natural effects. *Landscape and Urban Planning, 168*, 94–116. https://doi.org/10.1016/j.landurbplan.2017.09.019

Mallick, S. K., Das, P., Maity, B., Rudra, S., Pramanik, M., Pradhan, B., & Sahana, M. (2021). Understanding future urban growth, urban resilience and sustainable development of small cities using prediction-adaptation-resilience (PAR) approach. *Sustainable Cities and Society, 74*. https://doi.org/10.1016/j.scs.2021.103196

Nie, X., Lu, B., Chen, Z., Yang, Y., Chen, S., Chen, Z., & Wang, H. (2020). Increase or decrease? Integrating the CLUMondo and InVEST models to assess the impact of the implementation of the Major Function Oriented Zone planning on carbon storage. *Ecological Indicators, 118*. https://doi.org/10.1016/j.ecolind.2020.106708

OHUZP. (2020). Office of Housing and Urban - rural construction in Zhejiang Province). *Rainstorm intensity calculation criteria*. https://jst.zj.gov.cn/art/2020/3/6/art_1228990170_208.html (accessed 22 March 2022).

Oliveira Júnior, J. F., Correia Filho, W. L. F., Barros Santiago, D., Gois, G., Silva Costa, M., Silva Junior, C. A., Teodoro, P. E., & Freire, F. M (2021). Rainfall in Brazilian Northeast via in situ data and CHELSA product: mapping, trends, and socio-environmental implications. *Environmental Monitoring and Assessment, 193*, 263. https://doi.org/10.1007/s10661-021-09043-9

Oliveira Júnior, J. F., Correia Filho, W. L. F., Monteiro, L. S., Shah, M., Hafeez, A., Gois, G.d., Lyra, G. B., Carvalho, M. A., Barros Santiago, D., Souza, A., Mendes, D., Souza Costa, C. E. A., Blanco, C. J. C., Zeri, M., Pimentel, L. C. G., Jamjareegulgarn, P., & Silva, E. B (2022). Urban rainfall in the Capitals of Brazil: Variability, trend, and wavelet analysis. *Atmospheric Research, 267*. https://doi.org/10.1016/j.atmosres.2021.105984

Ornetsmüller, C., Verburg, P., & Heinimann, A. (2021). Scenarios of land system change in the Lao PDR: Transitions in response to alternative demands on goods and services provided by the land. *Applied Geography, 75*, 1–11. https://doi.org/10.1016/j.apgeog.2016.07.010

Pal, S. C., Chowdhuri, I., Das, B., Chakrabortty, R., Roy, P., Saha, A., & Shit, M. (2022). Threats of climate change and land use patterns enhance the susceptibility of future floods in India. *Journal of Environmental Management, 305*, Article 114317. https://doi.org/10.1016/j.jenvman.2021.114317

Paprotny, D., Sebastian, A., Morales-Napoles, O., & Jonkman, S. N. (2018). Trends in flood losses in Europe over the past 150 years. *Nature Communications, 9*, 1985. https://doi.org/10.1038/s41467-018-04253-1

Peng, H., Liu, Y., Wang, H., Gao, X., Chen, Y., & Ma, L. (2016). Urban stormwater forecasting model and drainage optimization based on water environmental capacity. *Environmental Earth Sciences, 75*. https://doi.org/10.1007/s12665-016-5824-x

Quan, R. (2018). Prediction of Land Use Change and Its Hydrological Effect in Shanghai Based on Scenario Simulation (in Chinese). *Journal of Natural Resources, 33*, 1552–1562. https://doi.org/10.31497/zrzyxb.20170858

Quan, R., Liu, M., Lu, M., Zhang, L., Wang, J., & Xu, S. (2010). Waterlogging risk assessment based on land use/cover change: a case study in Pudong New Area, Shanghai. *Environmental Earth Sciences, 61*, 1113–1121. https://doi.org/10.1007/s12665-009-0431-8

Rahnama, M. R. (2021). Forecasting land-use changes in Mashhad Metropolitan area using Cellular Automata and Markov chain model for 2016-2030. *Sustainable Cities and Society, 64*. https://doi.org/10.1016/j.scs.2020.102548

Ren, X., Hong, N., Li, L., Kang, J., & Li, J. (2020). Effect of infiltration rate changes in urban soils on stormwater runoff process. *Geoderma, 363*. https://doi.org/10.1016/j.geoderma.2019.114158

Shahzad, H., Myers, B., Boland, J., Hewa, G., & Johnson, T. (2022). Stormwater runoff reduction benefits of distributed curbside infiltration devices in an urban catchment. *Water Research, 215*. https://doi.org/10.1016/j.watres.2022.118273

Shrestha, S., Bhatta, B., Shrestha, M., & Shrestha, P. K. (2018). Integrated assessment of the climate and landuse change impact on hydrology and water quality in the Songkhram River Basin, Thailand. *Science of The Total Environment, 643*, 1610–1622. https://doi.org/10.1016/j.scitotenv.2018.06.306

Silva Cruz, J., Blanco, C. J. C., & Oliveira Júnior, J. F. (2022). Modeling of land use and land cover change dynamics for future projection of the Amazon number curve.

Science of The Total Environment, 811. https://doi.org/10.1016/j.scitotenv.2021.152348

Sofia, G., Roder, G., Dalla Fontana, G., & Tarolli, P. (2017). Flood dynamics in urbanised landscapes: 100 years of climate and humans' interaction. *Scientific Reports, 7*. https://doi.org/10.1038/srep40527

Song, J., Wang, J., Xi, G., & Lin, H. (2021). Evaluation of stormwater runoff quantity integral management via sponge city construction: A pilot case study of Jinan. *Urban Water Journal, 18*, 151–162. https://doi.org/10.1080/1573062X.2020.1860237

Stehfest, E., van Zeist, W. J., Valin, H., Havlik, P., Popp, A., Kyle, P., Tabeau, A., Mason-D'Croz, D., Hasegawa, T., Bodirsky, B. L., Calvin, K., Doelman, J. C., Fujimori, S., Humpenoder, F., Lotze-Campen, H., van Meijl, H., & Wiebe, K. (2019). Key determinants of global land-use projections. *Nature Communications, 10*, 2166. https://doi.org/10.1038/s41467-019-09945-w

Sterling, S. M., Ducharne, A., & Polcher, J. (2013). The impact of global land-cover change on the terrestrial water cycle. *Nature Climate Change, 3*, 385–390. https://doi.org/10.1038/nclimate1690

Stokes, E. C., & Seto, K. C. (2019). Characterizing urban infrastructural transitions for the Sustainable Development Goals using multi-temporal land, population, and nighttime light data. *Remote Sensing of Environment, 234*. https://doi.org/10.1016/j.rse.2019.111430

Van Asselen, S., & Verburg, P. (2013). Land cover change or land-use intensification: simulating land system change with a global-scale land change model. *Global Change Biology, 19*, 3648–3667. https://doi.org/10.1111/gcb.12331

Wagner, P. D., Bhallamudi, S. M., Narasimhan, B., Kumar, S., Fohrer, N., & Fiener, P. (2019). Comparing the effects of dynamic versus static representations of land use change in hydrologic impact assessments. In *Environmental Modelling and Software, 122*. https://doi.org/10.1016/j.envsoft.2017.06.023

Wang, H., Lu, S., Lu, B., & Nie, X. (2021). Overt and covert: The relationship between the transfer of land development rights and carbon emissions. *Land Use Policy, 108*. https://doi.org/10.1016/j.landusepol.2021.105665

Wang, H., Tao, R., Wang, L. L., & Su, F. B. (2010). Farmland preservation and land development rights trading in Zhejiang, China. *Habitat International, 34*, 454–463. https://doi.org/10.1016/j.habitatint.2009.12.004

Wang, Q., Xu, Y., Xu, Y., Wu, L., Wang, Y., & Han, L. (2018). Spatial hydrological responses to land use and land cover changes in a typical catchment of the Yangtze River Delta region. *Catena, 170*, 305–315. https://doi.org/10.1016/j.catena.2018.06.022

Wang, Y., van Vliet, J., Debonne, N., Pu, L., & Verburg, P. H. (2021). Settlement changes after peak population: Land system projections for China until 2050. *Landscape and Urban Planning, 209*. https://doi.org/10.1016/j.landurbplan.2021.104045

Willner, S. N., Otto, C., & Levermann, A. (2018). Global economic response to river floods. *Nature Climate Change, 8*, 594–598. https://doi.org/10.1038/s41558-018-0173-2

Winsemius, H. C., Aerts, J. C. J. H., van Beek, L. P. H., Bierkens, M. F. P., Bouwman, A., Jongman, B., Kwadijk, J. C. J., Ligtvoet, W., Lucas, P. L., van Vuuren, D. P., & Ward, P. J. (2016). Global drivers of future river flood risk. *Nature Climate Change, 6*, 381–385. https://doi.org/10.1038/nclimate2893

Wu, H., Lin, A., Xing, X., Song, D., & Li, Y. (2021). Identifying core driving factors of urban land use change from global land cover products and POI data using the random forest method. *International Journal of Applied Earth Observation and Geoinformation, 103*. https://doi.org/10.1016/j.jag.2021.102475

Xie, H., He, Y., & Xie, X. (2017). Exploring the factors influencing ecological land change for China's Beijing–Tianjin–Hebei Region using big data. *Journal of Cleaner Production, 142*, 677–687. https://doi.org/10.1016/j.jclepro.2016.03.064

Xu, C., Rahman, M., Haase, D., Wu, Y., Su, M., & Pauleit, S. (2020). Surface runoff in urban areas: The role of residential cover and urban growth form. *Journal of Cleaner Production, 262*. https://doi.org/10.1016/j.jclepro.2020.121421

Yang, L., Li, J., Zhou, K., Feng, P., & Dong, L. (2021). The effects of surface pollution on urban river water quality under rainfall events in Wuqing district, Tianjin, China. *Journal of Cleaner Production, 293*. https://doi.org/10.1016/j.jclepro.2021.126136

Zhang, H., Yang, Z., Cai, Y., Qiu, J., & Huang, B. (2021). Impacts of Climate Change on Urban Drainage Systems by Future Short-Duration Design Rainstorms. *Water, 13*. https://doi.org/10.3390/w13192718

Zhang, M., Xu, M., Wang, Z., & Lai, C. (2021). Assessment of the vulnerability of road networks to urban waterlogging based on a coupled hydrodynamic model. *Journal of Hydrology, 603*. https://doi.org/10.1016/j.jhydrol.2021.127105

Zhang, Q., Wu, Z., Zhang, H., Dalla Fontana, G., & Tarolli, P. (2020). Identifying dominant factors of waterlogging events in metropolitan coastal cities: The case study of Guangzhou, China. *Journal of Environmental Management, 271*, Article 110951. https://doi.org/10.1016/j.jenvman.2020.110951

Zhang, W., Wang, W., Li, X., & Ye, F. (2014). Economic development and farmland protection: An assessment of rewarded land conversion quotas trading in Zhejiang, China. *Land Use Policy, 38*, 467–476. https://doi.org/10.1016/j.landusepol.2013.12.008

Zhou, T., Liang, Q., & Wang, Y. (2021). Waterlogging risk assessment and comprehensive renovation scheme construction based on InfoWorks ICM model (in Chinese). *China Flood and Drought Management, 31*, 12–19. https://doi.org/10.16867/j.issn.1673-9264.2021105

Zhou, Y., Li, X., & Liu, Y. (2021). Cultivated land protection and rational use in China. *Land Use Policy, 106*. https://doi.org/10.1016/j.landusepol.2021.105454